JOURNAL OF PHYSICAL SCIENCE
ISSN: 1675-3402 (PRINT) 2180-4230 (ONLINE)

PENERBIT USM
PENYEBARAN ILMU MELALUI PENERBITAN

Vol. 33, No. 3 (2022)

Journal of Physical Science, Vol. 33(3), 63–79, 2022

Synthesis and Characterisation of Graphene Oxide/Chitosan Composite Membranes from Natural Waste

Andi Muhammad Afdhal Saputra,[1] Nadea Agustina,[1] Amran,[1] Zurnansyah,[1] Samnur[2] and Eko Hadi Sujiono[1*]

[1]Laboratory of Materials Physics, Department of Physics, Universitas Negeri Makassar, Makassar, 90224 South Sulawesi, Indonesia
[2]Department of Mechanical Engineering, Universitas Negeri Makassar, Makassar, 90224 South Sulawesi, Indonesia

[*]Corresponding author: e.h.sujiono@unm.ac.id

Published online: 30 November 2022

To cite this article: Saputra, A. M. A. et al. (2022). Synthesis and characterisation of graphene oxide/chitosan composite membranes from natural waste. *J. Phys. Sci.*, 33(3), 63–79. https://doi.org/10.21315/jps2022.33.3.5

To link to this article: https://doi.org/10.21315/jps2022.33.3.5

ABSTRACT: *In this paper, we report the synthesis and physical properties of the graphene oxide (GO) /chitosan (CS) composite membrane, which is effectively synthesised using natural waste. The GO/CS composite membrane analysis results were confirmed using XRD, FTIR and SEM. The XRD results of the GO/CS composite membrane showed that the diffraction peak of chitosan appeared at 2θ = 19.3° and the diffraction peak of GO appeared at 2θ = 26.3°, with the GO peak being dominant, which makes the crystallinity of CS decrease. The FTIR spectrum of the GO/CS membrane showed the disappearance of the CS glucopyranose band and the functional group (C=O) of GO at 891 cm^{-1} and 1,704 cm^{-1} and the functional group (C=C) of GO decreased at a wavelength of 1,557 cm^{-1}. The SEM results showed the surface morphology of the GO/CS membrane, where the surface of the GO/CS composite membrane became smooth due to the contact between the hydroxyl and NH groups in CS with oxygen-containing groups in GO. The XRD, FTIR and SEM results showed the physical interaction between GO and CS. They are increasing the value of Young's modulus, elasticity, elongation at break and absorption of metal ions. The GO/CS composite membranes are expected to have potential applications in metal absorption, biochemistry and electrochemistry.*

Keywords: graphene oxide, chitosan, composite, membrane, nanomaterials

1. INTRODUCTION

Composite materials are materials made from two or more integral materials with significantly different physical and chemical properties, which, when combined, produce materials with varying characteristics of the individual constituents. Currently, scientists are trying to find materials with good physicochemical properties in nanoscience and technology. For example, graphene has attracted much attention from scientists since it was first reported in 2004 due to its unique mechanical, electrical and quantum properties.[1] Compared to expensive fullerenes and carbon nanotube (CNT), graphene oxide (GO) or reduced graphene oxide (rGO) is way cheaper and easier to obtain. As a result, GO is predicted to be a new supporting filler for polymer, inorganic and metallic materials.

Based on the literature, it has been observed that GO shows excellent biocompatibility with high mechanical strength, so this material can be applied in various fields.[2] In addition, the oxygen-containing group on GO can be used as an active catalytic center to design covalent or non-covalent modifications according to the requirements of specific application fields. In addition, the presence of oxygen-containing groups also expands the GO interlayer gap, which can be activated by small molecules or polymer intercalation. Currently, significant progress has been made in the functionalisation of GO.[3]

Chitosan (CS), produced from chitin through the distillation process, is an environmentally friendly and renewable natural biopolymer with outstanding non-toxic, biocompatible and biodegradable properties.[4] In addition, many amino and hydroxyl groups, make CS efficiently absorb compounds, organic anions and metal ions through electrostatic or chelation interactions, which are widely applied in industrial, environmental (removal of heavy metal) and biomedical fields.[5,6] But, this natural biopolymer is generally used for tissue engineering, wound dressings and drug delivery.[7,8] However, the dense hydrogen bonds between amino and hydroxyl groups which are abundant in chitosan, have caused fundamental drawbacks such as low mechanical properties and poor solubility in standard solvents.

Many studies on GO/CS composites have shown that GO is an efficient nanofiller for strengthening CS to achieve better mechanical properties. Therefore, the combination of GO as a carbon material exhibits good biocompatibility with high mechanical strength. CS, a cationic polymer with dense hydrogen bonds but low mechanical properties, will make it possible to obtain nanocomposites with the desired properties.[9] On the other hand, the challenge is that GO does not mix well with organic polymers, so that does not produce a homogenous composite.[10]

However, some GO-reinforced CS materials are claimed to be potentially valuable as biomaterials. But so far, little work has been done on GO/CS composite membranes made from natural materials due to their incompatibility and others.

This study developed GO/CS membranes using natural materials derived from organic waste. For the synthesis of GO, we used coconut shells as the raw material, while for the synthesis of CS, we used shrimp shells. It was hoped that this natural material's GO/CS membrane could obtain the desired properties using X-ray diffraction (XRD), Fourier Transform Infrared (FTIR) and Scanning Electron Microscope (SEM), especially the physical and chemical properties. Meanwhile, this work is expected to offer a new way to manufacture GO/CS membranes from natural waste and to find the physical properties of GO/CS membranes from natural waste.

2. EXPERIMENTAL

2.1 Materials and Chemicals

The material of sodium hydroxide (NaOH), hydrochloric acid (HCl), potassium permanganate ($KMnO_4$), hydrogen peroxide (H_2O_2), sulphuric acid (H_2SO_4), sodium nitrate ($NaNO_3$), acetic acid (HAc), sodium silicate (Na_2SiO_3) were bought from CV Intraco, Makassar, Indonesia. The coconut shell was obtained from Gowa Regency in South Sulawesi, Indonesia. Meanwhile, the shrimp shells were obtained from Sidrap Regency in South Sulawesi, Indonesia.

2.2 Synthesis of Graphene Oxide (GO)

The synthesis of GO was accomplished by a modified hummer's method, as reported elsewhere.[11] The GO synthesis procedure was described as follows: Firstly, 1 g of graphite-based coconut shell and 0.5 g of $NaNO_3$ were mixed into 25 mL of H_2SO_4 and stirred for half an hour in an ice bath. Next, 3 g of $KMnO_4$ was added gradually to the solution, and the stirring process continued for 3 h. Then, 50 mL of deionised water was added slowly and stirred for 1 h. After that, the solution was separated from the ice bath and stirred continuously for 1 h while the temperature was maintained at 35°C.

Next, 100 mL of deionised water was added slowly and stirred for 1 h. After that, to remove the remaining $KMnO_4$, 5 mL of H_2O_2 solution was added slowly to the solution and then stirred for 30 min. Next, centrifugation was carried out to get the precipitate from the solution, and deionised water was added repeatedly until

the pH was 6–7. Finally, the precipitate obtained was heated in an oven at 110°C for 12 h to get GO powder. A schematic illustration of GO synthesis using the modified hummers method is shown in Figure 1.

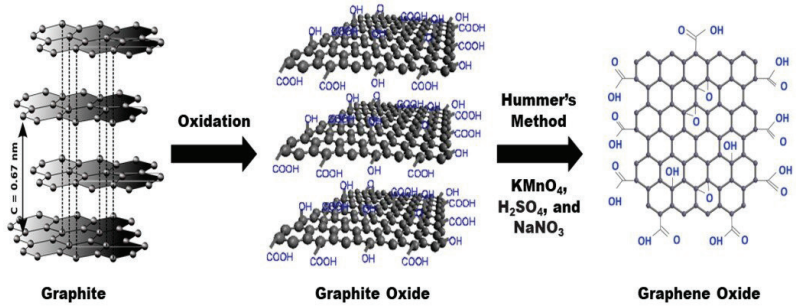

Figure 1: Schematic illustration of the synthesis of GO.

2.3 Synthesis of Chitosan (CS)

The basic material used in the CS synthesis process was shrimp shells. These shells were crushed into a fine powder. The first procedure was the deproteinisation process. This process was administered at a temperature of 75°C–80°C with 1 M NaOH solution, with a ratio of shrimp shells to NaOH = 1:10 (w/v), while stirring continuously for an hour. Furthermore, the filtrate obtained was washed using distilled water while waiting for the pH to be neutral. Next, the second procedure was the demineralisation process at a temperature of 25°C–30°C, using 2 M HCl solution with a ratio of sample and HCl solution = 1:10 (w/v) by stirring continuously for 2 h.

The next step was filtering, and the precipitate obtained was washed using distilled water until the pH was neutral. The product obtained is called chitin. The third procedure was the deacetylation process. The obtained chitin was added to a 20% NaOH solution while stirring continuously for 60 min at a temperature of 90°C–100°C. Finally, the obtained slurry was cleaned with distilled water until the pH was neutral and then dried to obtain chitosan powder.

2.4 Synthesis of GO/CS Composite Membrane

The method used preparation of GO/CS composites is the modified method established by Bagheripour et al.[12] Firstly, GO powder (0.5 g) was added to 100 mL of deionised water and ultrasonically stirred for a quarter of an hour (15 min) until a homogeneous solution was obtained. Next, 1 mL of HAc and 1 g of CS were added to the solution slowly while stirring.

Then, after 1 h of stirring at room temperature, 0.1 M NaOH was added gradually to obtain a neutral pH (6–7), followed by centrifugation using deionised water to obtain a precipitate. Finally, the precipitate obtained was heated in an oven for 12 h at 60°C to get GO/CS composite powder. The schematic illustration for the synthesis of the GO/CS composite is shown in Figure 2.

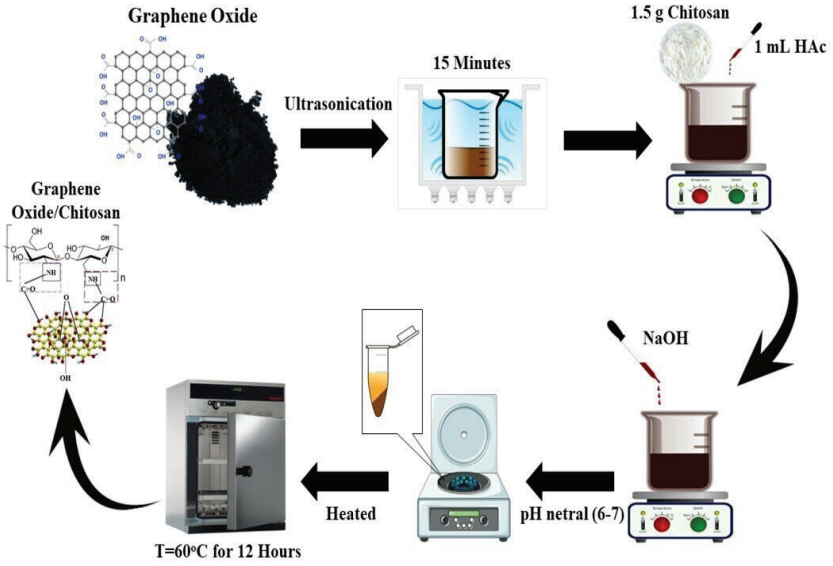

Figure 2: Schematic illustration for the synthesis of GO/CS composite.

The next stage was the synthesis of the membrane. Firstly, 3 g of Na_2SiO_3, 3 g of deionised water and 1.5 g of GO/CS composite powder were prepared. Next, GO/CS composite powder was heated at 120°C for 1 h. Then, to make the adhesive solution, distilled water and Na_2SiO_3 were mixed and stirred for 20 min at a temperature of 85°C. Next, after 20 min, 1.5 g of GO/CS composite powder were added to the adhesive solution and stir for 10 min. After stirring, the nylon filter was soaked in the solution for 10 min and then heated at 100°C for 1 h until a membrane was obtained.

2.5 Characterisation

XRD characterisation was obtained using a Shimadzu XRD 7000 diffractometer. XRD characterisation was used to detect and analyse the phase of the sample. FTIR spectroscopy was performed using the Thermo Scientific Nicolet iS10 instrument in the range of 4,000 cm^{-1}–500 cm^{-1} to classify functional groups of GO,

CS and GO/CS composite membranes. SEM characterisation was administered using JEOL 6510 LA with an operational voltage of 15 kV to obtain the surface morphology of GO, CS and GO/CS composite membranes.

3. RESULTS AND DISCUSSION

3.1 X-ray Diffraction (XRD) Analysis

The XRD spectrum of GO in Figure 3(a) shows the presence of two dominant peaks at angles of $2\theta = 23^{o}$ and 42.5^{o}, which shows the diffraction pattern of amorphous materials, as evidenced by the smooth and wide peaks without the appearance of sharpness, as found in the diffraction pattern of crystalline materials.[13] This result is different from Manna et al., which found that the strong diffraction peak of industrial GO was at 11^{o}.[14] However, similar results were reported by Sujiono et al., where two dominant peaks in GO based-coconut shells are a strong peak at 23^{o} and a small peak at 43^{o}.[11] These peaks experienced a shift indicating that the sample was in the rGO phase.[11,15] Several effects caused a shift in the diffraction pattern; firstly, because the precursor used in the synthesis came from natural waste (coconut shell), which was an amorphous material and secondly, because of changes in the degree of oxidation during the synthesis process.[11]

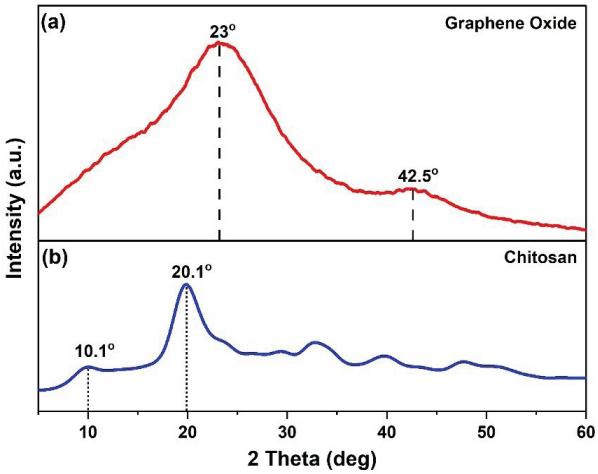

Figure 3: XRD pattern of (a) GO based-coconut shell (b) CS-based shrimp shell.

Figure 3(b) shows the XRD pattern of a polycrystalline CS sample, which offers a very sharp XRD reflection at 2θ = 10.1° and 20.1°, for peaks of 2θ = 20.1° indicating a high degree of crystallinity due to its amorphous shape.[16] The XRD pattern of CS based-shrimp shell sample was almost identical to the XRD pattern of commercial CS, as reported by Kumari et al. The strong XRD reflection peaks of commercial CS were at 20°, 45°, 65° and 75°.[17] However, similar results were obtained by several studies, such as those reported by Trung et al. and Ali et al., which found two specific diffraction peaks in shrimp shell CS samples with a small peak at 10° and a strong peak at 20°.[18,19]

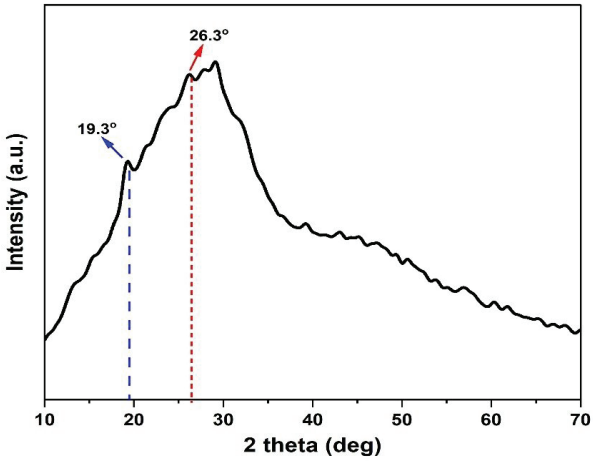

Figure 4: XRD pattern of the GO/CS membrane.

The XRD pattern of the GO/CS composite membrane can be seen in Figure 4. In the GO/CS composite membrane spectrum, CS's peak was shown at 2θ = 19.3°, which was associated with the amorphous state of CS, and the diffraction peak of GO appeared at 2θ = 26.3°.[5] The position of the XRD peak associated with CS is in close agreement with the literature reported by Le et al.[20] However, there was a difference in the peak of GO because the GO in this work experienced a shift in the rGO phase. The GO/CS membrane samples showed a more dominant GO peak than the CS peak, so the degree of CS crystallinity decreased after adding GO.[21] Additionally, the CS was evenly distributed in the GO matrix.[22] The more dominant GO distribution can increase the tensile strength of the GO/CS membrane, and the hydrogen bonds become stronger. This shows that the degree of crystallinity does not play an essential role in improving the mechanical properties, especially the tensile strength of GO/CS membranes.[23] However, according to Ali et al., the decrease in polymer crystallinity plays an essential role in increasing the absorption and capacity of metal ions.[19] In addition, the incorporation of GO and

CS occurred through physical interactions such as π-π accumulation, hydrogen bonding and van der Waals force rather than chemical interactions.[5] The physical interactions can improve physical properties, especially the value of Young's modulus, elongation at break and conductivity.[24]

The widening of XRD peaks in the GO/CS membrane samples occurred due to the sample's crystallite size and micro-strain contribution. Crystallite size and microstrain values were obtained using equations (1) and (2),[25,26] respectively:

The values for crystallite size were calculated using the Scherrer formula:

$$\beta_D = \frac{k_\lambda}{D \cos\theta} \quad (1)$$

Where,

β_D = the estimated crystallite size

D = the full width at half maximum (FWHM) of the peak

k = a constant (i.e., 0.94)

λ = the wavelength of the X-radiation (i.e., 0.154)

θ = the Bragg's angle.

And the values for microstrain were calculated using the following equation:

$$\beta_\varepsilon = \frac{n_2}{4 \tan\theta} \quad (2)$$

Where,

β_ε = the micro-strain

n_2 = the micro-deformation broadening

θ = the Bragg's angle.

Formula (1) and (2) are used to calculate the crystallite size and microstrain values of the GO/CS membrane sample. The results are given in Table 1.

Table 1: Details of the crystallite size and microstrain values of the GO/CS membrane.

Material	Peak Position (2θ)	Crystallite size (nm)	Micro-strain (x 10^{-1})	Index Crystallinity (%)
GO/CS	19.3°	9.36 nm	2.48	64.82
	26.3°	6.91 nm	2.22	

3.2 Fourier Transform infrared Analysis

The output obtained from FT-IR spectroscopy is a graph of the interaction of the peaks of molecules that absorb energy from the spectrum, which is shown by a diagram of the relationship between proportion (%T) and wavenumber (cm^{-1}).[11]

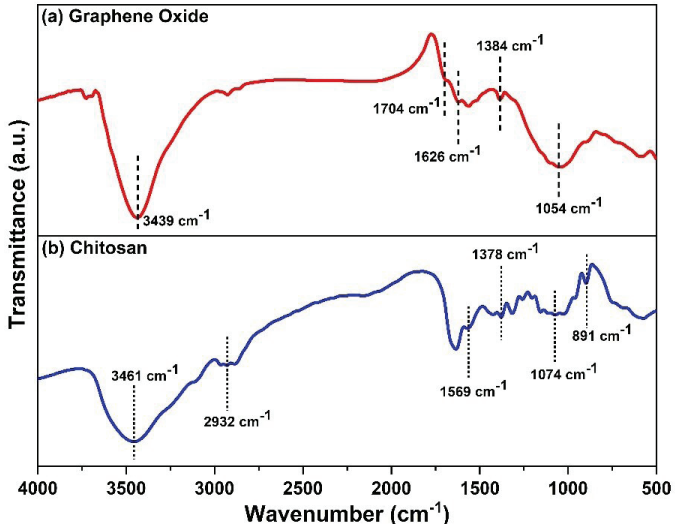

Figure 5: FTIR spectra of (a) GO-based coconut shell and (b) CS-based shrimp.

Figure 5(a) shows the absorption peak of the FTIR spectrum of GO. Five functional groups of oxygen-containing can be easily identified. A strong and broad absorption peak at 3,439 cm^{-1} was associated with stretching vibrations hydroxyl (-OH), the weak peak of the stretching vibration (C=O) at 1,704 cm^{-1}, the strong peak of aromatic (C=C) group at 1,626 cm^{-1},[11] a strong peak at 1,384 cm^{-1} was associated with alkoxy (C-O) vibrations and an epoxy group (C-O) identified at 1,054 cm^{-1}.[27] These results confirm that several functional groups contained oxygen, such as hydroxyl, carboxyl, alkoxy and epoxy.[11] A comparison of functional groups between GO-based coconut shell and GO synthesised from pure graphite reported by Mahmoodi et al.[27] can be seen in Table 2.

Table 2: The types of bonds (functional groups) present in GO-based coconut shell and GO-based pure graphite.

Peak	Bond types (Functional groups)	Wavenumber (GO-based Coconut Shell Waste) (cm^{-1})	Wavenumber (GO-based pure graphite) (cm^{-1}) [27]
1	-OH (Hydroxyl)	3,439	3,446
2	C=O (Carboxyl)	1,704	1,732
3	C=C (Aromatic)	1,626	1,624
4	C-O (Alkoxy)	1,384	1,392
5	C-O (Epoxy)	1,054	1,060

As seen in Figure 5(b), the FTIR peak for the CS based-shrimp shell was observed. The peak at 3,461 cm^{-1} (-OH angle deformation), 2,932 cm^{-1} (-CH stretching) and the peak at 1,644 cm^{-1} were associated with the stretching vibration of the carbonyl from the amino acetate group,[28] peaks at 1,569 cm^{-1} (bending vibrations of $-NH_2$ in the amino group), peak at 1,378 cm^{-1} (primary, secondary and tertiary bonds -NH), and peak at 1,074 cm^{-1} (C-O stretching in acetamide). The FTIR spectrum of CS that we report was almost similar to that reported by Kumari et al.[17]

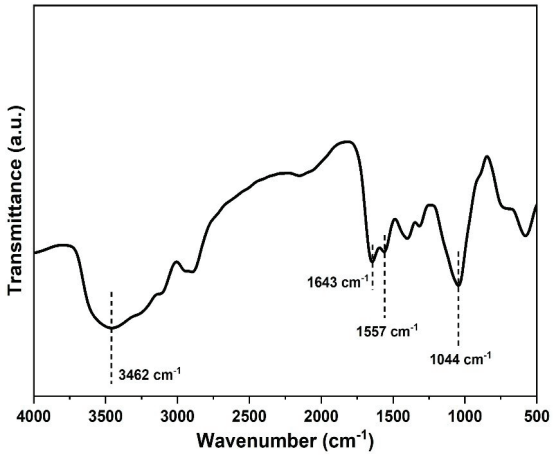

Figure 6: FTIR spectra of the GO/CS membrane.

The FTIR spectrum of the GO/CS membrane can be seen in Figure 6. Observation of the FTIR spectrum of the GO/CS membrane is noteworthy because there are several bands experiencing changes in intensity when compared to the FTIR spectrum of GO and CS. For example, the CS glucopyranose band at 891 cm^{-1} disappeared after combining GO with CS. Besides, the formation of an amide linkage between GO and CS is indicated by the disappearance of the functional group (C=O) at the peak of GO at 1,704 cm^{-1}, which NH_2 is caused by CS, which reacted with the C=O of GO.[29,30] The broad absorption band at 3,462 cm^{-1} was associated with a mixture of amino strains from CS and (-OH) from GO, the peak at 1,643 cm^{-1} indicated a carbonyl stretching vibration of the amino acetate group of CS, the peak at 1,557 cm^{-1} associated with a C=C from GO which experienced a decrease. The peak at 1,044 cm^{-1} represented (C-O) epoxy that of GO. The FTIR results show an interaction between CS and GO and almost have similarities to those reported by Jin et al.[28] The reaction mechanism between GO and CS can be seen in Figure 7, adapted from Suksompong et al.[30] The reaction mechanism explains that when GO is mixed with CS, an electrostatic interaction is formed between the C=O group of GO and the NH group of CS, resulting in GO/CS, which is stable with increased elasticity.[30,31] This statement is from the discussion of the XRD results, which states that GO's tensile strength (elasticity) increases when GO and CS are combined.

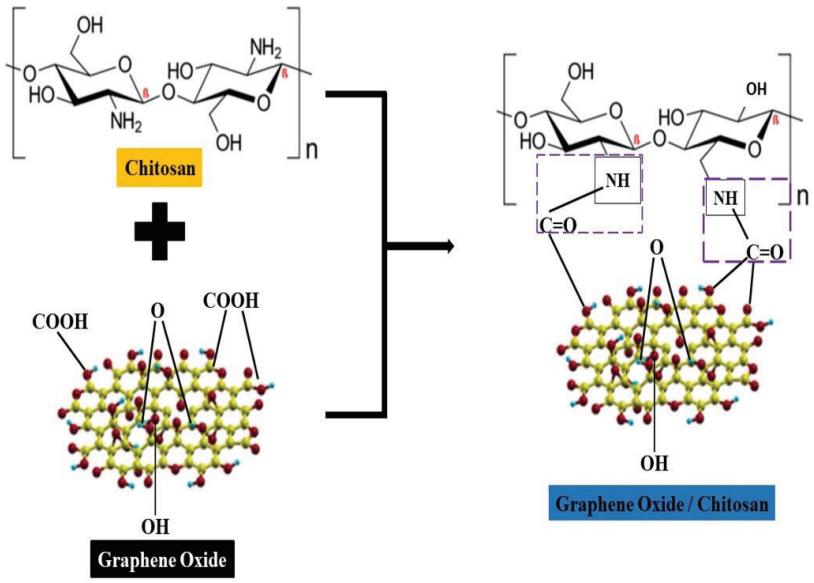

Figure 7: Depicts the reaction mechanism between GO and CS (Adapted from Suksompong et al.[30]).

3.3 Scanning Electron Microscopy (SEM) Analysis

The SEM image shows the surface morphology of the GO sample in Figure 8 (a). From the picture, it can be seen that the GO surface was rough, irregular and had a large surface area. In addition, the sample network structure shows a three-dimensional carbon network structure with different pore sizes.[11] Figure 8 (b) shows the results of the SEM image of the CS based-shrimp shell. It can be seen that the sample's surface has an irregular structure. In addition, the surface morphology of the sample had some parts that were smooth, rough and poreless.[32]

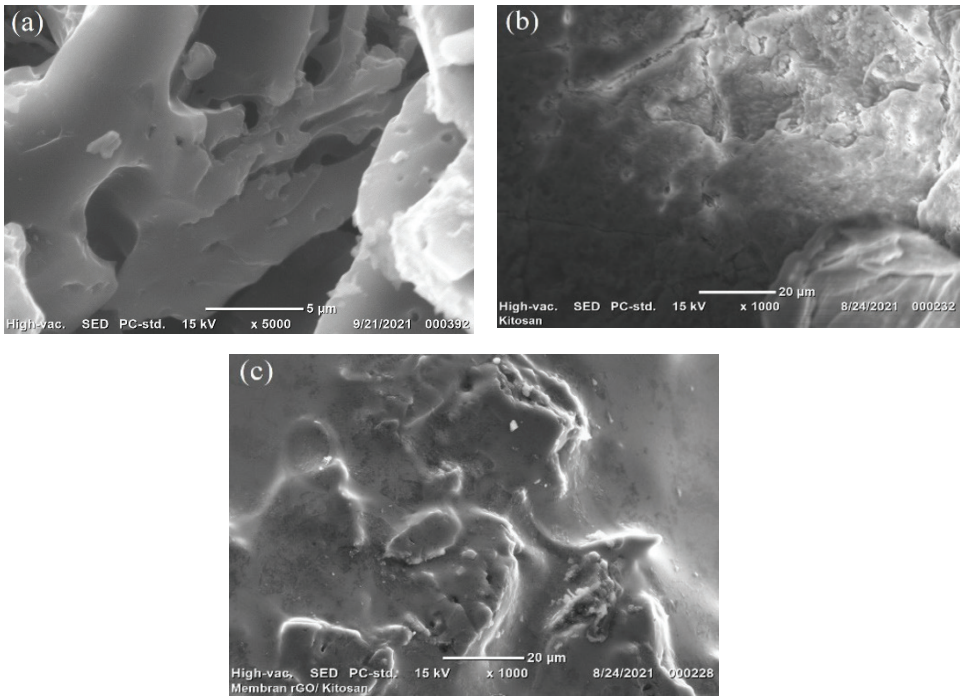

Figure 8: Surface morphology of (a) GO-based coconut shell, (b) CS-based shrimp shell, and (c) GO/CS membrane.

Figure 8(c) shows the surface morphology of the GO/CS membrane where the surface of the GO/CS membrane looked smoother and had no pores so that it could increase the tensile strength.[33] In addition, the membrane morphology showed a homogeneous and high distribution of GO in CS. This was due to the contact between the hydroxyl and NH groups in CS and oxygen-containing groups in GO. In addition, the physical interaction between GO and CS can increase the value of Young's modulus, thereby increasing the fracture strain.[11] Therefore, the combination of GO and CS can be used as a multifunctional material to be applied in the metal absorption, biochemical and electrochemical industries.

3.4 Method and Applications of GO/CS membrane composite

Generally, several methods are used for the fabrication of GO/CS composites, including solution methods, aerogel, hydrogel, electrospinning and wet spinning. In membrane manufacturing technology, particular emphasis is placed on hybrid composites and nanocomposite membranes. Membrane properties are influenced by the type of additive, additive concentration, pore size, pore distribution, polymer concentration and the fabrication method used.[34]

Previous studies reported several methods for making GO and CS membrane composites. Table 3 presents a list of GO/CS composites and their applications made by different processes. The method often used to make composites is the solution method. The solution mixing method in this study showed that the GO/CS composite membrane had a smooth surface, as shown in Figure 8(c), with GO being more dominant than CS. GO/CS composites can be made by various methods with varying results. For example, the aerogel method reported by Hao et al.[35] found that the composite morphology has a large surface area with uniform pore size. Similar results were obtained using the hydrogel method reported by Han and Yan,[36] which found that the GO/CS surface had many pores. Meanwhile, GO/CS composites have a large surface area and good mechanical properties using the electrospinning method.[37] Different results were obtained using the wet spinning method reported by Du et al.,[38] which found that the composite surface was very rough and the sheet was like a hump.

Table 3: Lists GO/CS composites and their applications made by different processes.

Material	Method	Results	Application	Ref.
GO, CS, Deionised Water	Aerogel	High surface area and uniform pore size distribution.	Supercapacitor electrode	35
GO, CS	Hydrogel	The surface had many pores, where noncovalent interactions occurred.	Biomaterials and smart materials	36
GO, CS, Polyvinyl Alcohol	Electrospinning	Excellent mechanical properties and a large surface area.	Tissue engineering and drug delivery	37
GO, CS, Silica, Hydrofluoric acid	Wet Spinning	The surface was very rough and the sheet was like a hump.	The removal of dyes from industrial wastewater	38
GO, CS	Solution Mixing	The surface area was smooth and poreless.	Not reported	This Work

GO/CS composite membrane is promising material because it has unique physical and chemical properties. The results and discussion on XRD, FTIR and SEM showed a good physical interaction between GO and CS that could increase the value of Young's modulus, elongation at break, elasticity and metal ion absorption.[39] In Table 3, there are several GO/CS composite applications, including supercapacitor electrodes,[35] biomaterials and smart materials,[36] tissue engineering and drug delivery and the removal of dyes from industrial wastewater.[37,38] Meanwhile, in our work, the GO/CS membranes were expected to have potential applications in the metal adsorption, biochemical and electrochemical industries.

4. CONCLUSION

This research made a GO/CS composite membrane using a simple method. The GO/CS membrane diffraction XRD peak showed a more dominant GO peak, so the degree of crystallinity in CS decreased. The SEM surface morphology of the GO/CS composite membrane was smooth because the distribution of GO in CS was good due to hydroxyl and NH groups in CS and oxygen-containing groups in GO. The FTIR results showed the disappearance of the C=O functional group in GO and the glucopyranose band in CS. In addition, the FTIR and XRD results have been confirmed because of an increase in tensile strength or elasticity on the GO/CS membrane. GO/CS membranes are expected to have potential applications for the metal absorption, biochemical and electrochemical industries.

5. ACKNOWLEDGEMENTS

The authors would like to thank Indonesia's Ministry of Education, Culture, Research and Technology through the Student Creativity Program–Exact Research in 2021.

Competing interest statement

The authors declare no conflict of interest.

6. REFERENCES

1. Banerjee, A. N. (2018). Graphene and its derivatives as biomedical materials: Future prospects and challenges. *Interface Focus*, 8(3). https://doi.org/10.1098/rsfs.2017.0056
2. Raucci, M. G. et al. (2017). Comparative facile methods for preparing graphene oxide–hydroxyapatite for bone tissue engineering. *J. Tissue Eng. Regen. Med.*, 11(8), 2204–2216. https://doi.org/10.1002/term.2119
3. Yu, W. et al. (2020). Progress in the functional modification of graphene/graphene oxide: A review. *RSC Adv.*, 10(26), 15328–15345. https://doi.org/10.1039/d0ra01068e
4. Jiménez-Gómez, C. P. & Cecilia, J. A. (2020). Chitosan: A natural biopolymer with a wide and varied range of applications. *Molecules*, 25(17), 3981. https://doi.org/10.3390/molecules25173981
5. Wu, K. et al. (2020). Fabrication of chitosan/graphene oxide composite aerogel microspheres with high bilirubin removal performance. *Mater. Sci. Engin. C*, 106, 110162. https://doi.org/10.1016/j.msec.2019.110162
6. Fouda-Mbanga, B. G. et al. (2021). Carbohydrate biopolymers, lignin based adsorbents for removal of heavy metals (Cd2+, Pb2+, Zn2+) from wastewater, regeneration and reuse for spent adsorbents including latent fingerprint detection: A review. *Biotechnol. Rep.*, 30, e00609. https://doi.org/10.1016/j.btre.2021.e00609
7. Liu, H. et al. (2018). A functional chitosan-based hydrogel as a wound dressing and drug delivery system in the treatment of wound healing. *RSC Adv.*, 8(14), 7533–7549. https://doi.org/10.1039/c7ra13510f
8. Ahsan, S. M. et al. (2018). Chitosan as biomaterial in drug delivery and tissue engineering. *Int. J. Biol. Macromol.*, 110, 97–109. https://doi.org/10.1016/j.ijbiomac.2017.08.140
9. Zhang, C. et al. (2018). Fabrication of reduced graphene oxide/chitosan composite fiber by dry-jet wet spinning. *Adv. Compos. Hybrid Mater.*, 1(2), 347–355. https://doi.org/10.1007/s42114-018-0029-2
10. Yilmaz Dogan, H. et al. (2022). Fabrication and properties of graphene oxide and reduced graphene oxide reinforced Poly(Vinyl alcohol) nanocomposite films for packaging applications. *Polym. Polym. Compos.*, 30. https://doi.org/10.1177/09673911221113328
11. Sujiono, E. H. et al. (2020). Graphene oxide-based coconut shell waste: synthesis by modified Hummers method and characterization. *Heliyon*, 6(8), e04568. https://doi.org/10.1016/j.heliyon.2020.e04568
12. Bagheripour, E. et al. (2018). Novel composite graphene oxide/chitosan nanoplates incorporated into PES based nanofiltration membrane: Chromium removal and antifouling enhancement. *J. Ind. Engin. Chem.*, 62, 311–320. https://doi.org/10.1016/j.jiec.2018.01.009

13. Yunarti, R. T. et al. (2022). Facile synthesis of composite between titania nanoparticles with highly exposed (001) facet and coconut shell-derived graphene oxide for photodegradation of methylene blue. *J. Phys. Chem. Solids*, 160, 110357. https://doi.org/10.1016/j.jpcs.2021.110357
14. Manna, S. et al. (2019). Synthesis of graphene oxide nano-materials coated bio-char using carbonaceous industrial waste for phenol separation from water. *Colloids Surf. A Physicochem. Eng. Asp*., 581, 123818. https://doi.org/10.1016/j.colsurfa.2019.123818
15. Liu, G. et al. (2015). A reduced graphene oxide modified metallic cobalt composite with superior electrochemical performance for supercapacitors. *RSC Adv*., 5(78), 63553–63560. https://doi.org/10.1039/C5RA09748G
16. Bagheri, R. et al. Characterization, antioxidant and antibacterial activities of chitosan nanoparticles loaded with nettle essential oil. *J. Food Meas. Charact.*, 15(2), 1395–1402. https://doi.org/10.1007/s11694-020-00738-0
17. Kumari, S. et al. (2017). Physicochemical properties and characterization of chitosan synthesized from fish scales, crab and shrimp shells. *Int. J. Biol. Macromol*., 104, 1697–1705. https://doi.org/10.1016/j.ijbiomac.2017.04.119
18. Trung, T. S. et al. (2020). Improved method for production of chitin and chitosan from shrimp shells. *Carbohydr. Res*., 489, 107913. https://doi.org/10.1016/j.carres.2020.107913
19. Ali, M. E. A. et al. (2018). Chitosan nanoparticles extracted from shrimp shells, application for removal of Fe(II) and Mn(II) from aqueous phases. *Sep. Sci. Technol.*, 53(18), 2870–2881. https://doi.org/10.1080/01496395.2018.1489845
20. Le, T. T. N. et al. (2019). Preparation of magnetic graphene oxide/chitosan composite beads for effective removal of heavy metals and dyes from aqueous solutions. *Chem. Eng. Commun*., 206(10), 1337–1352. https://doi.org/10.1080/00986445.2018.1558215
21. Shah, J. et al. (2018). Magnetic chitosan graphene oxide composite for solid phase extraction of phenylurea herbicides. *Carbohydr. Polym*., 199, 461–472. https://doi.org/10.1016/j.carbpol.2018.07.050
22. Zhang, L. et al. (2021). Structure and properties of graphene oxide-chitosan composite membrane prepared by the plasma acid solvent. *J. Fiber Sci. and Technol.*, 74(6), 143–149. https://doi.org/10.2115/fiberst.2018-0020
23. Yang, X. et al. (2010). Well-dispersed chitosan/graphene oxide nanocomposites. *ACS Appl. Mater. Interfaces*, 2(6), 1707–1713. https://doi.org/10.1021/am100222m
24. Wang, X. et al. (2010). Electrically conductive and mechanically strong biomimetic chitosan/reduced graphene oxide composite films. *J. Mater. Chem*., 20(41), 9032–9036. https://doi.org/10.1039/c0jm01852j
25. Dhayal, V. et al. (2020). Spectroscopic studies, molecular structure optimization and investigation of structural and electrical properties of novel and biodegradable Chitosan-GO polymer nanocomposites. *J. Mater. Sci*., 55(30), 14829–14847. https://doi.org/10.1007/s10853-020-05093-5

26. Mohamad Zaidi, U. Z. et al. (2019). Crystallite size and microstrain: XRD line broadening analysis of AgSiN thin films. *Pigm. Resin Technol.*, 48(6), 473–480. https://doi.org/10.1108/PRT-03-2018-0026
27. Mahmoodi, H. et al. (2021). Graphene oxide-chitosan hydrogel for adsorptive removal of diclofenac from aqueous solution: Preparation, characterization, kinetic and thermodynamic modelling. *RSC Adv.*, 11(57), 36289–36304. https://doi.org/10.1039/d1ra06069d
28. Jin, X. et al. (2019). High strength graphene oxide/chitosan composite screws with a steel-concrete structure. *Carbohydr. Polym.*, 214, 167–173. https://doi.org/10.1016/j.carbpol.2019.03.039
29. Sabzevari, M. et al. (2018). Graphene oxide-chitosan composite material for treatment of a model dye effluent. *ACS Omega*, 3(10), 13045–13054. https://doi.org/10.1021/acsomega.8b01871
30. Suksompong, T. et al. (2021). Efficacy of a graphene oxide/chitosan sponge for removal of radioactive iodine-131 from aqueous solutions. *Life*, 11(7). https://doi.org/10.3390/life11070721
31. Emadi, F. et al. (2017). Functionalized graphene oxide with chitosan for protein nanocarriers to protect against enzymatic cleavage and retain collagenase activity. *Sci. Rep.*, 7, 1–13. https://doi.org/10.1038/srep42258
32. Eddya, M. et al. (2020). A comparison of chitosan properties after extraction from shrimp shells by diluted and concentrated acids. *Heliyon*, 6(2), e03486. https://doi.org/10.1016/j.heliyon.2020.e03486
33. Han, D. et al. (2011). Preparation of chitosan/graphene oxide composite film with enhanced mechanical strength in the wet state. *Carbohydr. Polym.*, 83(2), 653–658. https://doi.org/10.1016/j.carbpol.2010.08.038
34. Kausar, A. (2019). Applications of polymer/graphene nanocomposite membranes: A review. *Mater. Res. Innov.*, 23(5), 276–287. https://doi.org/10.1080/14328917.2018.1456636
35. Hao, P. et al. (2015). Graphene-based nitrogen self-doped hierarchical porous carbon aerogels derived from chitosan for high performance supercapacitors. *Nano Energy*, 15, 9–23. https://doi.org/10.1016/j.nanoen.2015.02.035
36. Han, D. & Yan, L. (2014). Supramolecular hydrogel of chitosan in the presence of graphene oxide nanosheets as 2D cross-linkers. *ACS Sustain. Chem. Eng.*, 2(2), 296–300. https://doi.org/10.1021/sc400352a
37. Liu, Y. et al. (2014). Facile preparation and characterization of poly(vinyl alcohol)/chitosan/graphene oxide biocomposite nanofibers. *J. Ind. Engin. Chem.*, 20(6), 4415–4420. https://doi.org/10.1016/j.jiec.2014.02.009
38. Du, Q. et al. (2014). Highly enhanced adsorption of congo red onto graphene oxide/chitosan fibers by wet-chemical etching off silica nanoparticles. *Chem. Engin. J.*, 245, 99–106. https://doi.org/10.1016/j.cej.2014.02.006
39. Yuan, L. et al. (2021). Chitosan based antibacterial composite materials for leather industry: a review. *J. Leather Sci. Engin.*, 3(1). https://doi.org/10.1186/s42825-020-00045-w